PHYSICAL REVIEW B VOLUME 25, NUMBER 2 15 JANUARY 1982

Specific heat of glasses at low temperatures

Arup K. Raychaudhuri* and R. O. Pohl
Laboratory of Atomic and Solid State Physics, Cornell University, Ithaca, New York 14853

(Received 21 August 1981)

We have studied the specific heat of nitrate glasses ($T < 1$ K) doped with water, lithium, and nitrite. We have found that there is a basic difference between doped crystals and doped glasses regarding the excess specific heat caused by the presence of the dopants. Dopants in glasses cause a change in the low-temperature specific heat only if the glass transition temperature T_G changes upon admixing. The excess specific heat is found to be inversely proportional to T_G. Similar results have been observed on silica containing sodium and on neutron-irradiated silica, for which the important parameter is the fictive temperature T_f. It is concluded that the frozen-in disorder in the glass, which is measured by T_G (or T_f), is an important factor in determining the density of states of low-energy excitations which are characteristic of the amorphous state.

I. INTRODUCTION

Low-temperature properties of glasses ($T < 1$ K) have been studied extensively in recent years.[1] Thermal, acoustic, dielectric, and other measurements indicate the presence of a broad spectrum of low-energy two-level systems (TLS) in glasses. A phenomenological tunneling model[2,3] seems to explain the important observations. However, not much is known yet about the nature of the tunneling entities.

Tunneling of impurity atoms and molecules in crystalline solids has been well studied and most of its aspects are well understood.[4] The tunneling motion of impurity species gives rise to low-frequency excitations ($\tilde{\omega} \approx 1\ \text{cm}^{-1}$). They can be of rotational type as in RbCl:CN or KCl:NO_2 or off-center type as in KCL:Li or NaBr:F. It has been suggested that atoms or groups of atoms in glasses can undergo similar tunneling motions. There is, however, one important difference. In crystalline systems, it is the impurity which tunnels, whereas in glasses, the tunneling is believed to be intrinsic, i.e., the atoms which make the glass matrix take part in the tunneling motion.

The present search owes its origin to the above studies. The basic question that we asked is related to a very fundamental yet generally not well-recognized problem: whether it is at all possible for a molecular or atomic species in an amorphous solid to tunnel in the way it does in a crystalline matrix. In a crystal, the impurity has to fit inside a cage of well-defined shape; one has a potential for tunneling if the cage is loose enough. In a glass, the matrix may well form a tight fit around any shape or size impurity atom and never allow it to tunnel as a separate entity. It is known from studies of tunneling in crystals that not all impurities in crystals give rise to tunneling modes. Only a few selected impurities can tunnel in certain crystal matrices. There is no *a priori* way of predicting which impurity will tunnel in which matrix. Thus, the question arises whether there is any *a priori* reason why individual atoms or molecules will tunnel in an amorphous solid, and whether such tunneling is possible in all amorphous solids. If the TLS were indeed the result of tunneling by individual atoms or molecules then one might expect that tunneling should be readily produced by additional atomic or molecular species introduced deliberately into the glass. This study has been undertaken to do a systematic search for tunneling states in doped glasses. Previous studies by Stephens[5] and Lasjaunias[6] have shown that impurities, probably water, do increase the low-temperature specific heat, although the changes were small and no clear correlation between impurity concentration and specific heat anomaly was observed. (Note that changes in specific heat have been observed from iron contamination in glasses, but they result from spin states, not from tunneling.) Our study started with the following objectives.

(1) Into a single host glass try to incorporate impurity ions which are generally known to give rise to tunneling in crystals and then study how they

affect various properties of the glass.

(2) Try to establish scaling of changes, observed after doping, with impurity concentration.

(3) Compare and contrast it with the impurity modes in crystalline solids.

For these studies we have chosen an ionic glass made from $Ca(NO_3)_2$ and KNO_3.[7,8] The reasons for the choice are the following.

(1) The chemicals are easily available in pure form.

(2) Low melting point makes the preparation easy.

(3) The bonds in the glass are predominantly ionic[7] and the material may well serve as an amorphous counterpart for ionic crystals in which most of the studies on tunneling in crystals have been made. Dopants used were H_2O, Li^+, and NO_2^-.

We have also investigated the silica glasses, which had either been neutron irradiated or to which sodium oxide had been added.

II. EXPERIMENTAL TECHNIQUE

A. Preparation of nitrate glasses

Nitrate glasses were prepared using $Ca(No_3)_2 \cdot 4H_2O$ and KNO_3 as starting materials. Both materials are available commercially as reagent grade. For all the glasses in which doping studies were made we started with $\frac{2}{5}$ parts (by weight) of KNO_3 and $\frac{3}{5}$ parts (by weight) of $Ca(NO_3)_2 \cdot 4H_2O$. The melting batch varied in total weight from 40 to 100 g, depending on the need. The weighing was done to better than 1% accuracy. The mixture was heated in an open glass tube in a furnace with automatic temperature control. To start the meltdown the furnace was kept at 150–170 °C. When the liquid started bubbling water vapor was released. The temperature was then raised in a controlled way by steps of 20 °C. The temperature was raised only when bubbling at a certain temperature had ceased. In this fashion the melt was heated up to 400–500 °C to drive off most of its water. The melt then was extremely clear, but showed no sign of further evaporation or of decomposition, although it had a slight yellowish tint above 400 °C. Beyond 500 °C the melt cannot be heated because the nitrate starts decomposing into nitrite, which generally shows up as a faint brownish fume, and tiny bubbles appear in the melt. Careful control was absolutely necessary at this state. After the heating had been stopped and the tube taken out of the furnace, it was cooled in air for 5 min, and its contents poured into aluminum molds (both air-cooled and water-cooled molds work equally well). Upon cooling, a clear, plasticlike solid had formed.

By weight, $\frac{2}{5}$ part of KNO_3 and $\frac{3}{5}$ part of $Ca(NO_3)_2 \cdot 4H_2O$, when boiled together to drive off water, result in a glass of the composition 51 wt. % $Ca(NO_3)_2$ and 49 wt. % KNO_3. It is known[7] that the glass which contains 50.4 wt. % $Ca(NO_3)_2$ is as stable against crystallization as the more stable glasses in the system Na_2O-SiO_2. This weight composition corresponds to 39.1 mol % $Ca(NO_3)_2$ and 60.9 mol % KNO_3 and lies close to the middle of the glass formation range of the KNO_3-$Ca(NO_3)_2$ system (40–70 mol % KNO_3). This particular composition is one of the well-studied compositions of the nitrate glass family and will be henceforth referred to as 40/60 $Ca(NO_3)_2$-KNO_3.

Much effort was devoted to the removal of the residual water. The starting batch has ~18 wt. % water in it [from the $Ca(NO_3)_2 \cdot 4H_2O$]. Initially we attempted to dry the $Ca(NO_3)_2 \cdot 4H_2O$ at 100 °C in a vacuum, but this was inadequate. We then placed the whole system in a glove box and bubbled dry nitrogen or argon through it. By this method the water level was decreased to ~0.03 wt. %. It was not possible to go below this level mainly because of decomposition of the nitrate. To prevent decomposition we tried to bubble dry oxygen through the melt but it did not improve the situation. We then found that, although dry gas bubbling enhanced the rate of release of water of the melt, simply heating the melt up to 400–500 °C can lower the water level to ~0.05 wt. %, and produces a particularly clear glass. Since bubbling dry gas in a glove-box atmosphere is rather complicated, we decided to follow the simpler procedure of boiling in air.

The water concentration was monitored through ir absorption at 2.6, 1.92, and 1.44 μm. For glasses containing more water, the absorption at 2.6 μm was so large that it was difficult to obtain a sufficiently thin sample. For these glasses the concentration was monitored through the 1.92- and 1.44-μm bands. A sample cell shown in the inset of Fig. 1 was used. Sapphire windows were selected for their good transmission in this spectral range.

The spectrum was taken in a Cary 17 D spectrometer. A typical spectrum is shown in Fig. 1. Since the water concentration of our samples was

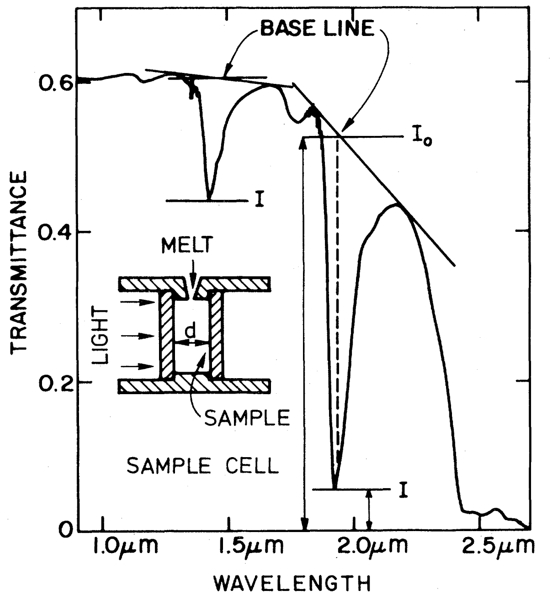

FIG. 1. Typical spectrum of a water containing nitrate glass. The absorption constant is given as $\alpha = (1/d)\ln(I_0/I)$, where d is the thickness of the sample. The inset shows the sample cell, made of aluminum, with sapphire windows.

changed over a wide range, the absorption band at 1.44 μm was the only one which could be kept on scale over the entire concentration range studied, using a sample thickness of 0.5 cm. A fixed-thickness sample cell helps to intercompare spectra without errors arising from thickness measurements. The bands were calibrated first by measuring the spectrum of 40/60 $Ca(NO_3)_2$-$KNO_3 \cdot 4H_2O$ glass. For samples with intermediate water contents, the concentration was determined through weight loss upon drying. As shown in Fig. 2, the peak absorption (α_m) for all three bands increases linearly with water concentration. The half-width of the absorption curve at 2.6 μm, which is the fundamental stretching vibration, is 280 cm^{-1} independent of water concentration. At the 2.6-μm band the absorption is 120 cm^{-1}/wt. % water. This is very close to the value of 100–50 cm^{-1}/wt. % water observed in silica-based glasses.[9]

Doping of the nitrate glass with water was done by controlling the boiling time and temperature. By this method a desired amount of water can be left in the melt before it is quenched to form a glass. The amount of water in the sample was then determined spectroscopically.

Hydroxyl doping was tried using KOH. Since KOH readily converts into K_2CO_3 by absorbing CO_2 from the atmosphere, the following procedure had to be used. A measured quantity of dry glass was mixed with a measured quantity of KOH in a beaker. The KOH was kept under ether during weighing. The mixture was then evacuated, melted in argon, and quenched. In spite of all the precautions taken, the sample turned out to be milky, probably because of carbonate. Very little OH^- was detected through ir absorption. The procedure was not pursued further.

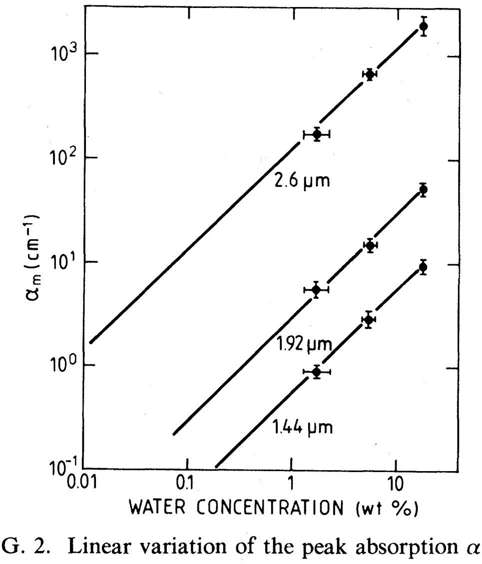

FIG. 2. Linear variation of the peak absorption α_{max} with the water concentration at 2.6, 1.92, and 1.44 μm.

Nitrite doping was done by adding a known amount of KNO_2 to the melt. To check whether the KNO_2 dissolved in the melt, a chemical test was performed based on a colorimetric method.[10] The nitrite was reacted with a primary aromatic amine in an acidic solution (in our case, 0.5 wt. % sulfanilamide in 20 vol % HCl) to form intermediate diazonium salt. The diazonium salt, when treated with an aromatic compound containing amino or hydroxyl substitutents, forms a conjugated azodye that is suitable for colorimetric measurements. The final product has an absorption band at 540–550 nm. This absorption was calibrated using a standard aqueous solution of KNO_2.

The value of the NO_2^- concentration obtained by this analysis agreed to better than 10% with the amount of NO_2^- added to the melt. By chemical analysis we found that the undoped material contains $\sim 4 \times 10^{19}$ NO_2^- ions/cm^3, which we suspect to come from the decomposition of nitrate during heating. Maximum doping achieved with KNO_2 was $\sim 5 \times 10^{20}/cm^3$. At higher concentrations, the samples became milky.

Lithium doping was done by adding measured quantities of $LiNO_3$ to the melt. The amount of Li^+ ions in the glass was checked by flame spectroscopy and found to be equal to the amount of Li calculated from the added $LiNO_3$. The maximum doping that we achieved was $\sim 6\times 10^{20}/cm^3$. At higher concentrations, a clear glass was not obtained.

B. Determination of T_G

The glass transition temperatures T_G of all the samples studied were determined by using a Dupont Thermal Analyzer. We used a heating rate of 10 K/min, which was approximately the cooling rate during quenching. Typical accuracy of T_G was ± 1 K. The data were reproducible within that accuracy and, for dry 40/60 nitrate glass, agreed with those determined by Angell and co-workers.[11] In Li^+- and NO_2^--containing glasses, an endothermic peak sometimes occurred just below T_G in the thermal analyzer curve, which we suspect to be caused by partial crystallization or by relaxation.

C. Specific-heat measurements

The specific heat (C_v) was determined in the temperature range 0.1–2.0 K using a heat-pulse technique described in detail elsewhere.[12] Here we mention only two important features.

The method consists of connecting the sample to the heat sink by a thermal link whose time constant is very large compared to the internal equilibrium time constant of the sample. Typically, the internal equilibrium constant of the sample was ~ 0.4 and ~ 0.2 sec at 0.1 and 1 K, respectively.

A heat pulse of definite power and time duration was applied, and the sample thermometer was monitored as a function of time. The sample relaxed to the temperature of the heat sink in an exponential fashion as shown in Fig. 3. In the log-linear plot of the time-temperature profile we always obtained a single straight line indicating an exponential decay with a single-time constant, τ_2. This indicated that the thermal link to the bath was the only factor which determined the time constant. This means that the specific heat was time independent on the time scale of our measurements. A typical variation of τ_2 with temperature is shown in Fig. 4.

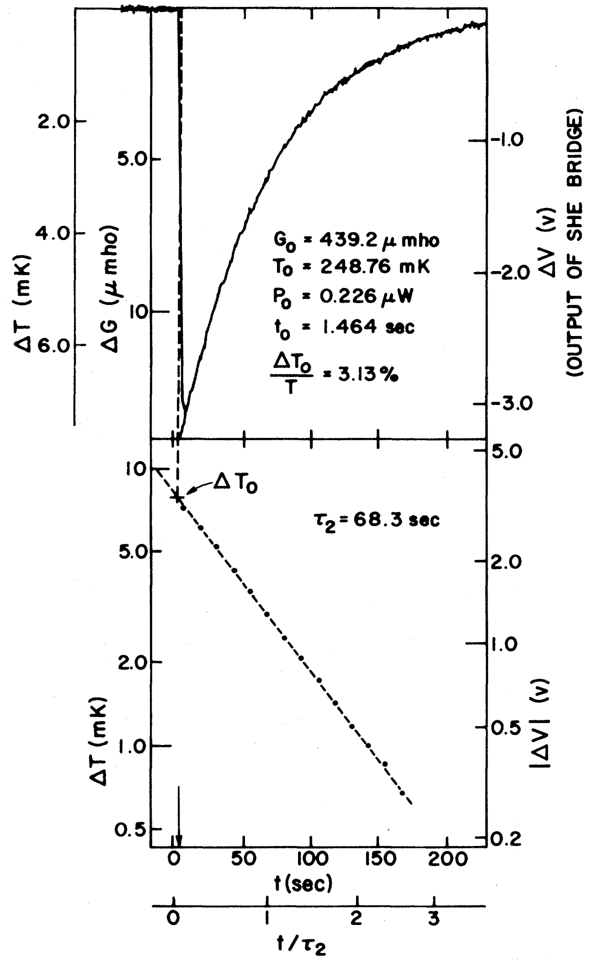

FIG. 3. A typical time-temperature profile obtained in specific-heat measurements. The lower curve shows the single-time-constant behavior. G_0 is the conductance of the carbon thermometer of equilibrium. Conductance bridge is SHE Corp. Model PCB.

The exponential decrease of the temperature rise after the application of the heat pulse of duration t_0 and power P_0 is given by an expression of the form[12]:

$$\Delta T(t) = \frac{\tau_2 P_0}{C_s}(e^{t_0/\tau_2}-1)e^{-t/\tau_2} \text{ for } t >> t_0 , \quad (1)$$

when the addenda heat capacity is negligible (in our case $\sim 2\%$ at 0.1 K, decreasing at higher temperature), and also when the thermometer-to-sample boundary resistance is smaller than the sample-to-bath thermal resistance. In Eq. (1), C_s is the sample heat capacity, and τ_2 is the time constant of the exponential decay given by $R_L C_s$,

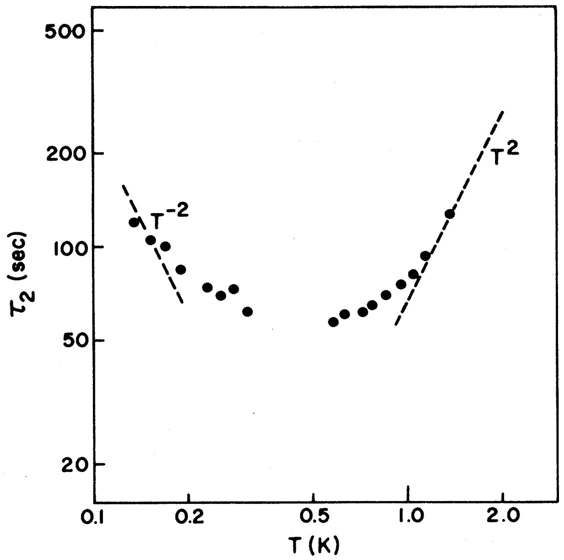

FIG. 4. A typical variation of sample-to-bath time constant is τ_2 with temperature.

where R_L is the sample-to-bath thermal resistance.

If Eq. (1) is evaluated at a time $t = t_0/2$ [where it actually does not describe the experimental $\Delta T(t)$], we obtain

$$\Delta T_0 = \frac{2\tau_2 P_0}{C_s} \sinh\left[\frac{t_0}{2\tau_2}\right] . \tag{2}$$

Typically, $\tau_2 > 50$ sec and $t_0 \lesssim 1.4$ sec, so $t_0 << 2\tau_2$. Thus, Eq. (2) can be approximated as

$$\Delta T_0 \approx P_0 t_0 / C_s . \tag{3}$$

Thus by extrapolating the observed long-time temperature profile back to the time $t = t_0/2$, as shown in Fig. 3, and not to $t = 0$, as one might perhaps assume, we can determine C_s using Eq. (3).

III. RESULTS

In Fig. 5 we show the specific heat C_v of a dry 40/60 $Ca(NO_3)_2$-KNO_3 glass. The low-temperature part ($T < 0.4$ K) follows a power law of the type $C_v = aT^b$, with $b = 1.33$ and $a = 90$ when C_v is expressed in the units erg/g K and T in K. For $T > 1.5$ K, C_v follows a T^3 relation with a coefficient 120 erg/g K^4. The Debye contribution to the T^3 specific heat has a coefficient 97.6 erg/g K^4 determined from sound velocity measurements.[5] The power-law variation of C_v for $T < 0.4$ K is typical for glasses. In Fig. 6 we show the specific heat of KNO_2 and $LiNO_3$ doped nitrate glass [40/60 $Ca(NO_3)_2$-KNO_3]. As can be seen, there is no change in the specific heat after doping with 5×10^{20} NO_2^- ions/cm^3 and 6×10^{20} Li^+ ions/cm^3. To investigate the extent to which the specific heat is unchanged, we calculated

$$\frac{\Delta C_v}{C_v} = \frac{(C_{\text{obs}} - C_{\text{calc}})}{C_{\text{calc}}}$$

(where $C_{\text{calc}} = 90 \times T^{1.33}$), for the undoped nitrate glass and also for the Li^+-doped and NO_2^--doped nitrate glass. $\Delta C_v / C_v$ is plotted in Fig. 7, which

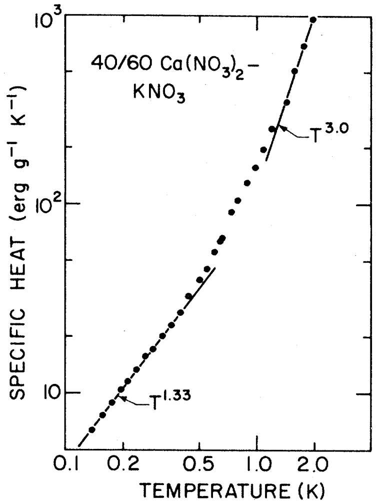

FIG. 5. Specific heat of dry 40/60 nitrate glass.

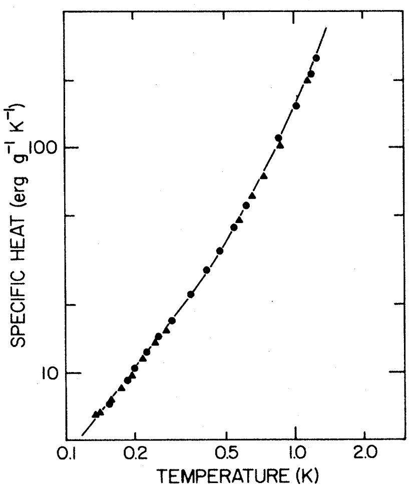

FIG. 6. Specific heat of Li^+- (circle) and NO_2^-- (triangle) doped 40/60 nitrate glass. The solid curve represents the specific heat of undoped glass (see Fig. 5).

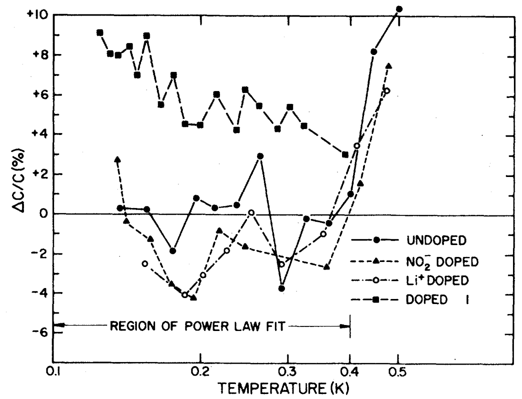

FIG. 7. Deviation of specific heats of undoped and of Li$^+$-, NO$_2{}^-$-, and H$_2$O-doped (doped 1) nitrate glasses from the best fit to undoped glass ($C_v=90T^{1.33}$). See text.

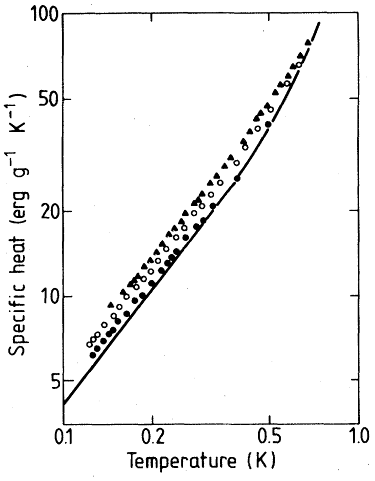

FIG. 8. Specific heats of water containing nitrate glasses. Solid line: undoped. Solid circle: doped 1; open circle: doped 2; triangles: doped 3. Data for doped 4 is not shown for clarity. Refer to Table I for details.

shows the scatter in our data as a deviation from the power-law fit. The specific heats of Li$^+$- and NO$_2{}^-$-doped glasses may be slightly lower than those of undoped glass by about 2%, with no systematic difference between the specific heats of Li$^+$- and NO$_2{}^-$-doped glasses within the scatter of the data. We do not attach any importance to this 2% difference. Firstly, the scatter in our data is of the order of $\pm 2\%$, and secondly, the slight difference could well result from variations in the relative contribution of the addenda which had not been subtracted. (The Li$^+$- and NO$_2{}^-$-doped samples had about 20% more mass than the undoped glasses.) Rather, we believe that these three sets of data serve as a test of the reproducibility of our data.

In Fig. 8 we have plotted the specific heat of water containing nitrate glasses, which we have labeled as doped 1 (with 1×10^{21} molecules/cm^3 or 1.6 wt. % water), doped 2 (2.5×10^{21} molecules/cm^3 or 3.4 wt. % water), and doped 3 (3.8×10^{21} molecules/cm^3 or 5.4 wt. % water). As can be seen, there is a distinct, though small, change in specific heat.

Since the doped 1 sample has a specific heat which is very close to that of the undoped glass, we have also plotted in Fig. 7 the percentage deviation of the specific heat, $\Delta C_v/C_v$, from that of the undoped glass. Thus, it can be seen that the specific heat of sample 1 clearly exceeds that of the water-free samples.

Previously,[5] the specific-heat data below 1 K were fitted to a relation of the type $C_v=C_1T+C_3T^3$. Lacking a proper theory, we have no *a priori* reason to choose between the two forms of fit; namely, the power-law or polynomial fits. Improvement of the quality of our data has given us the opportunity to resolve the issue at least experimentally. In Fig. 9 we have plotted C_v/T against T^2. At higher temperatures, straight lines can be drawn through the data points, but at lower temperatures significant deviations occur. In light of this it seems that a power-law description of the specific heat ($T<0.4$ K), as first suggested by Lasjaunias[6] for B$_2$O$_3$, may be the more appropriate description. In Fig. 10 we have plotted the specific heat of the undoped glass and of three doped samples after subtracting the Debye contribution, C_D, calculated from the sound velocity measured for

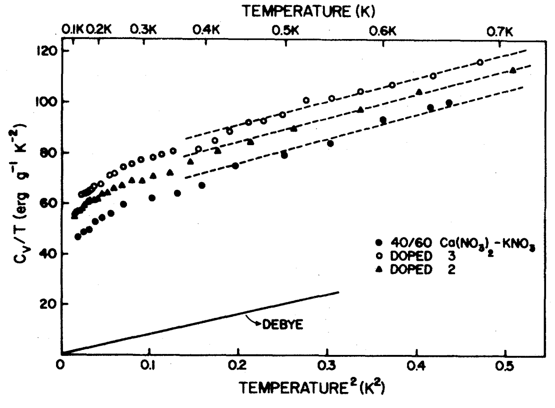

FIG. 9. Specific heats of undoped and doped glasses, plotted to check validity of the relation $C_v=C_1T+C_3T^3$. See text.

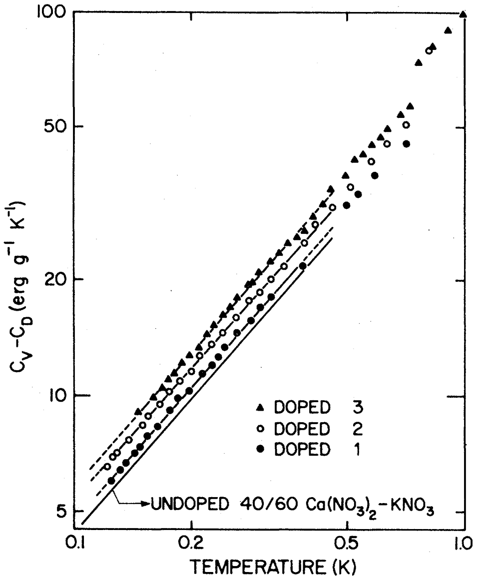

FIG. 10. Excess specific heats of doped and undoped glasses, obtained after subtracting Debye contribution from the observed specific heats.

the water-free sample. The data for sample 4 have been omitted for clarity. As can be seen, $(C_v - C_D) \propto T^n$ for all four glasses. All four straight lines are nearly parallel and the values of n for the individual straight lines do not show any systematic variation. The average value of $n = 1.156$. (Subtracting the Debye contribution only affects the higher-temperature data, and extends the straight-line fit in Fig. 10 beyond 0.4 K. Hence, the expected variation of C_D resulting from different speeds of sound in the water-doped samples is irrelevant at this point.)

In Fig. 11 we have plotted $a_{\text{exc}} = (C_v - C_D)/T^{1.156}$ against T for all the four glasses. The data for sample 4 have again been omitted for clarity. As can be seen, a_{exc} is almost constant over a wide temperature range (from 0.1 to 0.7 K). a_{exc} has been taken as the measure of excess specific heat of the glassy state. For convenience, the unit of a_{exc} is written as erg/g K^2. It implies that if T is in K, $C_v - C_D$ is in erg/g K. In Fig. 11, the arrows at the left-hand ordinate give the average value of a_{exc} (the average has been taken up to 0.4 K) and the bars give the standard deviation. The results are summarized in Table I. Figure 12 shows the scaling between a_{exc} and the water concentration in the nitrate glass. The quantity plotted is $\Delta a_{\text{exc}} = a_{\text{exc}}(\text{doped}) - a_{\text{exc}}(\text{undoped})$, i.e., the increase of the specific heat caused by the water doping.

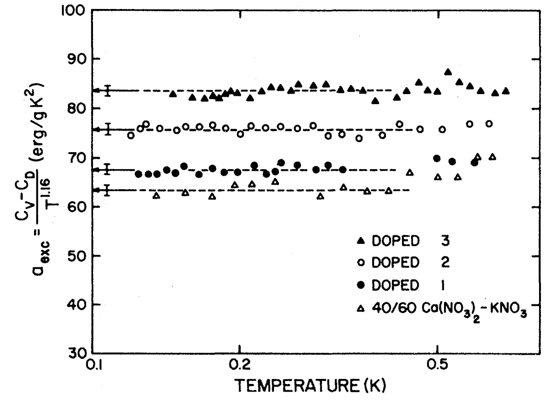

FIG. 11. Power-law fits to the extra specific heats of doped and undoped glasses.

IV. DISCUSSION

The data shown in Fig. 12 immediately suggest associating the increase of a_{exc},

$$\Delta a_{\text{exc}} = a_{\text{exc}}(\text{doped}) - a_{\text{exc}}(\text{undoped}) , \tag{4}$$

with some low-energy motional states of the water molecules dissolved in the glass. In that case, the total excess entropy

$$S = \int_0^{T'} \frac{1}{T}[C_v(\text{doped}) - C_v(\text{undoped})]dT \tag{5}$$

should be equal to (assuming two-level states)

$$S = nk_B \ln 2 , \tag{6}$$

where n is the concentration of the water molecules and k_B is Boltzmann's constant. T' is the maximum temperature to which the excess specific heat persists. In our experiments, it became unob-

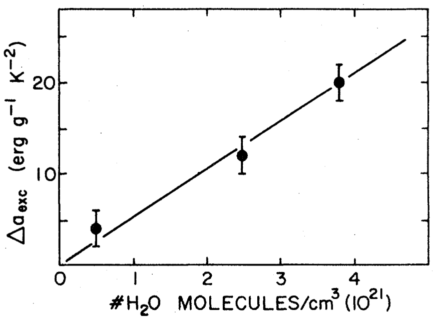

FIG. 12. Scaling of Δa_{exc} with water concentration. $\Delta a_{\text{exc}} = a_{\text{exc}}(\text{doped}) - a_{\text{exc}}(\text{undoped})$.

TABLE I. Glass transition temperatures, doping levels, and excess specific heat of doped and undoped nitrate glasses.

	40/60 $Ca(NO_3)_2$-KNO_3 nitrate glass							
	Undoped	Water doped 1	Water doped 2	Water doped 3	Water doped 4	Li^+ doped	NO_2^- doped	50/50 nitrate glass
T_G (K)	337	310	295	284	288	338	337	358[c]
Doping level molecules/cm^3		1.1×10^{21}	2.4×10^{21}	3.8×10^{21}	3.3×10^{21}	6×10^{20}	4.4×10^{20}	
a_{exc}[a]	63.3 ± 1.0	67.4 ± 1.0	75.7 ± 1.0	83.3 ± 1.0	80.0 ± 1.0	b	b	54 ± 5[d]

[a] Unit of a_{exc} is such that $C_{\text{exc}}=C_v-C_D$ is in erg g^{-1}K^{-1}. $C_{\text{exc}}=a_{\text{exc}}T^n$, $n\approx1.16$.
[b] Same as undoped glass, see Figs. 6 and 7.
[c] Determined by Williams and Angell, Ref. 11.
[d] Determined by Stephens, Ref. 5.

servable above approximately 0.7 K (see Fig. 8), and we will use this as T'. However, our conclusions are qualitatively unchanged even if a higher T' ($<T_{\text{melting}}$) is assumed.

As a representative case we consider sample 3. From the experimentally observed S we obtain $n=2.5\times10^{17}$ states/cm^3, which is 4 orders of magnitude lower than the number of added molecules (3.8×10^{21} molecules/cm^3). So we find that although Δa_{exc} scales with the water concentration, there is no one-to-one correspondence of the number of states estimated through S and the number of dissolved water molecules. This is to be contrasted with the tunneling of atoms and molecules in crystals,[4] where one has found such a correspondence. In our case, at the most only one out of 10^4 water molecules could be tunneling. For Li^+ and NO_2^- this fraction would have to be much smaller yet (although the T' is unknown).

When the dopant concentration in crystalline systems reaches $\sim10^{19}-10^{20}$ molecules/cm^3, one starts seeing the effect of impurity-impurity interaction which gives rise to a $T^{3/2}$ specific heat.[13] This concentration is much lower than the concentration of doping used here, and yet we do not see any change in temperature dependence. Another example of tunneling in crystalline systems which should be mentioned here is NaBr:F.[14] This system has a very broad (strain-induced) distribution of tunneling states, much akin to the distribution assumed in the tunneling model proposed for glasses.[2,3] This system also shows a linear heat capacity below 0.5 K, which satisfies Eq. (6) for fluorine concentrations varying from 9×10^{16}/cm^3 to 5.5×10^{18}/cm^3.

These comparisons show that there exists a basic difference between tunneling in doped crystals and tunneling of dopants in glasses (if there is any). On the other hand, the tunneling model has been very successful in explaining many phenomena observed in glasses. Hence one might postulate that the dopants in glasses cannot form individual tunneling entities, but rather they attach themselves to already existing two-level systems. With that picture one could understand the observed changes in dielectric properties[15] (if the dopants themselves carry a dipole) but changes in other properties would probably be small.

It is, conceivably, inappropriate to separate the doped glass into a "host" and a "dopant." When one dopes a glass, the resulting material may probably be more appropriately described as a different glass. Thus, the addition of foreign atoms may cause changes in other important properties of the glass. Such a change has actually been observed and will be described next. A brief description of the results has been published before.[16] We have found that the glass transition temperature in the nitrate glasses decreases with increasing water concentration (see Table I). This is not uncommon in many glass-forming systems.[17] In addition, however, we discovered that a connection exists between the glass transition temperature T_G and the excess specific heat. In Fig. 13 we have plotted a_{exc} measured from low-temperature calorimetry against $1/T_G$ for the undoped 40/60 nitrate glass and the four water-doped glasses. In the same graph we plotted one point which was obtained by Stephens on a dry sample with a different K:Ca concentration.[5] The T_G for this composition has

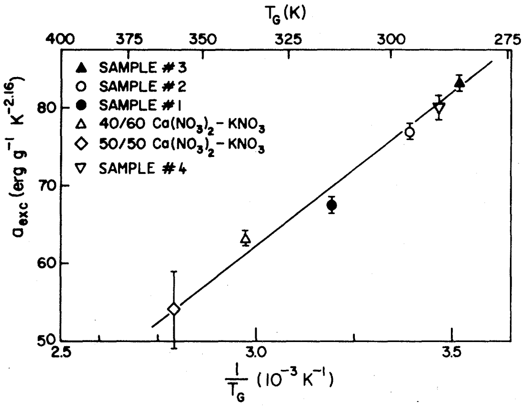

FIG. 13. Variation of $a_{\mathrm{exc}}=(C_v-C_D)/T^{1.16}$ in CaK-nitrate glass with glass transition temperature T_G. Water-doped samples are the same symbols as in Fig. 8. Open triangle: water-free sample. Inverted triangle: doped 4. See Table I.

been determined by Angell and co-workers.[11] Inspection of Fig. 13 shows that a_{exc} is related to T_G through a relation of the type

$$a_{\mathrm{exc}} \propto T_G{}^{-n}, \quad n \approx 1 \; . \tag{7}$$

Note that the results obtained on the Li^+- and $NO_2{}^-$-doped samples, i.e., no change of a_{exc} and no change of T_G, also agree with the relation expressed in Eq. (7).

In order to explore the generality of the connection between a_{exc} and T_G, we also investigated vitreous silica. In this system it is the fictive temperature that can be changed by neutron irradiation as well as by admixing other oxides. The fictive temperature T_f can be thought of as the temperature of the liquid whose disorder is the same as the frozen-in disorder of the glass as revealed, for instance, through mass-density fluctuation measured through small-angle x-ray scattering.[18] Thus, T_f carries similar information as T_G and in well annealed or slowly cooled glasses, $T_G \approx T_f$.[19,20] Figure 14 shows the specific heat of silica, neutron-irradiated silica, and soda silica. A summary of the data, including the fictive temperatures for these glasses, is contained in Table II. Figure 15 shows that a linear relationship of the form of Eq. (7) also holds for these glasses when T_G is replaced by T_f. We have plotted the data by normalizing T_f with $T_{f,0}$ which we identified to be 1475 K, and which is the T_G of the pure, unirradiated silica. This way we removed the uncertainty in determining the absolute values of T_f from the intensity of small-angle x-ray scattering.

Measurements on B_2O_3 glasses have provided at least qualitative evidence for a relation of the form of Eq. (7). It has been observed that the addition of water to B_2O_3 increases its specific heat,[5,6] while studies by Corsaro[21] on dry and wet B_2O_3 glasses have shown that the addition of water to B_2O_3 decreases its T_G. Unfortunately, the amount of water in the B_2O_3 glasses used in these measurements was not known, and therefore a quantitative comparison cannot be made at this time.

Encouraged by these observations, we tried to explore whether a relationship of the form of Eq. (7) holds generally for all glasses. In Fig. 16 we

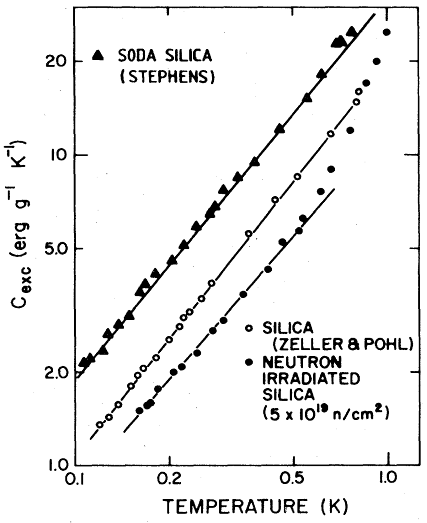

FIG. 14. Excess specific heat (C_v-C_D) of silica, neutron-irradiated silica, and soda silica. See Table III.

TABLE II. Fictive temperatures and excess specific heat of silica system.

	Vitreous silica	Irradiated vitreous silica	Soda silica
$\frac{T_{f,0}{}^{a}}{T_f}$	1	0.41	1.96
C_{exc}	$20T^{1.27}$	$12.3T^{1.16}$	$32.8T^{1.23}$
($\mathrm{erg\,g^{-1}K^{-1}}$)	b		c

[a] Obtained from intensity of small angle x-ray scattering, Ref. 18. $T_{f,0}=1475$ K $=T_G$ of annealed silica.

[b] From R. C. Zeller and R. O. Pohl, Phys. Rev. B 4, 2029 (1971).

[c] R. B. Stephens, Phys. Rev. B 8, 2896 (1973).

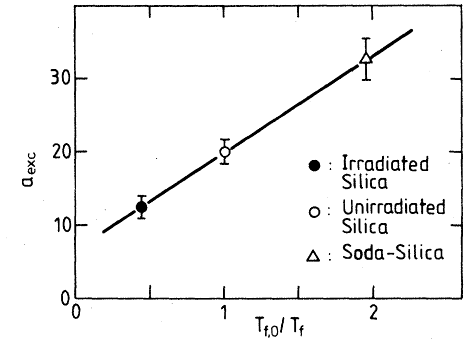

FIG. 15. Variation of a_{exc} for silica, neutron-irradiated silica, and soda silica. For SiO$_2$ $T_f = T_{f,0} = 1475$ K. See Table II. $a_{exc} = (C_v - C_D)/T^n$. C_v in units of erg g^{-1} K^{-1}.

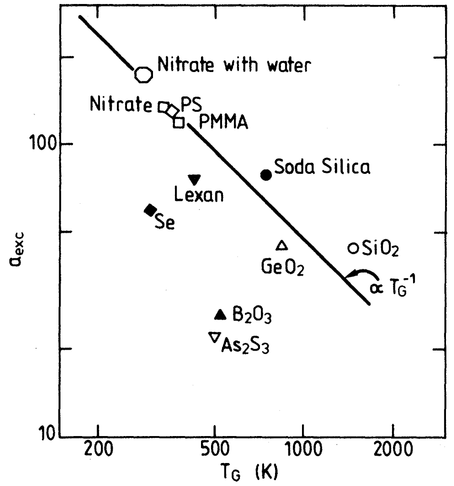

FIG. 16. a_{exc} for various glasses and their glass transition temperatures. Specific-heat data (except that of nitrate glasses) are from Ref. 5. See Table III. Note that a_{exc} is expressed, in this figure only, per unit volume. The line is $a_{exc} = 4.8 \times 10^4 / T_G$ (erg cm^{-3} K^{-1}).

have plotted all the data available on various glass-forming systems (see also Table III). It is at once clear that a single relation of the form of Eq. (7) does not hold. This complexity, however, is probably to be expected since we are comparing glasses of widely varying chemical composition and nature. Nevertheless, we found before that for glasses of similar chemical composition a relation of the form of Eq. (7) holds. Polymers like polystyrene, polymethylmethacrylate, and lexan polycarbonate could possibly belong to one group of glasses for which an expression of the form of Eq. (7) also holds. If we leave aside the three glasses Se, As$_2$S$_3$, and B$_2$O$_3$ for the time being, which show wide variations, for the remaining eight glasses an expression $a_{exc} \propto 4.8 \times 10^4 / T_G$ may hold with variations $\pm 30\%$ from the average, although this may be an accident. Taking all the data in Fig. 16 together, all we can say is that there appears to be a general trend that an increase in T_G is associated with a decrease of the specific-heat anomaly.

We will try to understand some of the implications of the observation that in glasses of similar chemical composition a correlation exists between the excess specific heat and the glass transition

TABLE III. Glass transition temperatures and excess specific heat of various glasses.

	SiO$_2$	GeO$_2$	0.25 Na$_2$O 0.75 SiO$_2$	B$_2$O$_3$	As$_2$S$_3$	Lexan polycarbonate	PMMA	PS	Nitrate	Se	Nitrate with water
T_G (K)[a]	1475	853	753	525	500	423	374	355	337	300	284
a_{exc}[b]	44	45	79	26	22	76	120	130	133	60	175
$a_{exc}T_G$ ($\times 10^{-4}$)	6.5	3.9	6.0	1.4	1.1	3.2	4.5	4.6	4.5	1.8	4.97

[a] Except for As$_2$S$_3$, lexan polycarbonate, and nitrate glasses, the rest of the glass transition temperatures have been obtained from C. L. Reynolds, Jr., J. Non-Cryst. Solids 30, 371 (1979). T_G for As$_2$S$_3$ was obtained from Ref. 7, for lexan polycarbonate from M. Breitling and J. H. Magill, J. Appl. Phys. 45, 4167 (1974). For nitrate glasses we used our own measurements (undoped and doped 3).

[b] a_{exc} is defined as $a_{exc}T^n = C_v - C_D$, $n = 1.2-1.3$ for most glasses. C_v is denoted in the unit of erg/cm^{3}K. There is no common basis for expressing the specific heats for glasses with wide variations in chemical nature. The choice of unit volume as the basis may be arbitrary but it contains the least uncertainties and is obtained directly from experiment. We refer to the following article for a discussion on this issue: C. A. Angell and W. Sichina, Ann. N. Y. Acad. Sci 279, 53 (1976).

temperature. A simple way of looking at the problem is to consider T_G (or T_f) as the determining factor for the energy scale of the problem. The configurational states which show up as the low-energy two-level states may be thought to be distributed over an energy range whose upper limit is determined by T_G. In that case, if a fixed number N of configurational states in a certain glass were distributed in some form over this energy range, the coefficient $a_{\rm exc}$ would be proportional to (N/k_BT_G). In a given glass-forming system (similar to those we have considered) it may be assumed that N is constant. In that case an inverse scaling of $a_{\rm exc}$ with T_G can be understood. It may be said that T_G plays the same role for the excess specific heat of a glass as that played by the Debye temperature for the lattice specific heat of crystals.

An upper limit of the energy scale equal to k_BT_G is an important ingredient of our picture. It is interesting to note that a similar picture has been proposed by Kastner and co-workers,[22,23] albeit in a very different context. In studying photoluminescence in amorphous SiO_2, Se, and As_2S_3 they noticed that the decrease in photoluminescence intensity ($I_{\rm PL}$) with increasing temperature could be described with a universal curve if a reduced temperature scale, T/T_G, was used, i.e.,

$$I_{\rm PL} \propto e^{-T/T_G} . \tag{8}$$

It is interesting to note that for neutron-irradiated silica, Eq. (8) was found not to describe the experimental data. However, as we discussed above, it is not T_G, but T_f which measures the disorder in neutron-irradiated silica. From the neutron fluence used by Kastner *et al.* ($\sim 10^{19}/{\rm cm}^2$) we estimate a $T_f \approx 1.5T_G$ for the irradiated silica, where T_G is the glass transition temperature for the unirradiated silica.[20] By using this value of T_f, rather than T_G of unirradiated silica in Eq. (8) we found that even for the neutron-irradiated silica, Eq. (8) describes the data well. This observation emphasizes the importance of the disorder in determining the temperature dependence of the photoluminescence in glasses.

To explain Eq. (8), Kastner[23] proposed a model in which the nonradiative process rate ν_{nr} is thought to arise from a thermally activated process across a barrier of height Δ, i.e.,

$$\nu_{nr} = \nu_0 e^{-\Delta/k_BT} ,$$

where $\nu_0 \approx 10^{13}$ Hz. The temperature dependence of $I_{\rm PL}$ can then be explained if a distribution of Δ of the following form is assumed:

$$g(\Delta) = \frac{1}{k_BT_G} e^{-\Delta/kT_G} . \tag{9}$$

Equation (9) means that the energy scale of the barrier-height distribution is determined by T_G. This is essentially the same conclusion as reached by us, although from entirely different experiments. It is still to be seen whether the photoluminescence centers can be associated with the two-level systems seen in low-temperature thermal or acoustic experiments, and what the possible connection is between the barrier heights discussed by Kastner and the energy splitting we are studying. Nevertheless, these two different experiments point to the fact that the energy scale over which different configurations in a glass are distributed is determined by T_G (or T_f), i.e., by the frozen-in disorder in the amorphous structure.

To get complete information on $a_{\rm exc}$, we need to know N, the total number of frozen-in configurations. For that we need a theory of glass transition which also gives a way to estimate N. Recently, Cohen and Grest[24,25] have proposed a free-volume theory of glass transition, which answers some of these questions. According to this theory, in a glass there exists free volume which is frozen in, as the liquid is cooled through T_G. This free volume can be distributed without expenditure of energy. Molecular diffusion takes place when accumulation of free volume may lead to formation of ephemeral voids of size v_m required for molecular species. As the glass is cooled, these ephemeral voids become long-lived vacancies. According to this theory, tunneling consists of the motion of a molecule bounding the void, into the void. This is thought of as the origin of TLS in glasses. The scale of the tunneling barriers is set by the maximum curvature of the free-energy surface, which is given by kT_G itself. Thus the theory provides the first physical picture for the connection between $a_{\rm exc}$ and T_G reported in this paper.

ACKNOWLEDGMENT

The authors want to thank J. De Yoreo and T. Klistner for specific-heat measurements of one of the samples. Dr. D. Ast of the Materials Science and Engineering Department, Cornell University, kindly provided the Dupont Thermal Analyzer. The help of G. Schmidt of the Cornell Materials

Science Center in glass preparation is acknowledged. One of us (R.O.P.) wants to thank Professor F. Pobell for his hospitality at the Institut für Festkörperforschung der Kernforschungsanlage Jülich during completion of this manuscript. This work was supported by the National Science Foundation under Grant No. DMR-78-01560 and through the facilities of the Cornell Materials Science Center.

---

[*] Present address: Max-Planck-Institut für Festkörperforschung, Heisenberg Str. 1, 7000 Stuttgart 80, West Germany.

[1] *Amorphous Solids: Low Temperature Properties,* edited by W. A. Phillips (Springer, New York, 1981).

[2] W. A. Phillips, J. Low Temp. Phys. 7, 351 (1972).

[3] P. W. Anderson, B. I. Halperin, and C. M. Varma, Philos. Mag. 25, 1 (1972).

[4] V. Narayanamurti and R. O. Pohl, Rev. Mod. Phys. 42, 201 (1970).

[5] R. B. Stephens, Phys. Rev. B 13, 852 (1976).

[6] J. C. Lasjaunias, A. Ravex, and M. Vandorpe, Solid State Commun. 17, 1045 (1975).

[7] H. Rawson, *Inorganic Glass Forming Systems* (Academic, New York, 1967).

[8] L. G. van Uitert and W. H. Grodkiewicz, Mater. Res. Bull. 6, 283 (1971).

[9] J. Paul Williams, Yao-Sin Su, W. R. Strzegowski, B. L. Butler, H. L. Hoover, and V. O. Altemose, Bull. Am. Ceram. Soc. 55, 141 (1976).

[10] C. A. Streuli and R. P. Averell, *The Analytical Chemistry of Nitrogen and its Compounds* (Wiley-Interscience, New York, 1970).

[11] E. Williams and C. A. Angell, J. Phys. Chem. 81, 3 (1977); K. J. Rao, D. B. Helphrey, and C. A. Angell, Phys. Chem. Glasses 14, 26 (1973).

[12] A. K. Raychaudhuri, Ph.D thesis, Cornell University, 1980 (unpublished), Cornell Materials Science Center Report #4284, August 1980.

[13] A. T. Fiory, Phys. Rev. B 4, 614 (1971).

[14] R. J. Rollefson, Phys. Rev. B 5, 3235 (1972).

[15] M. von Schickfus and S. Hunklinger, J. Phys. C 9, L439 (1976).

[16] A. K. Raychaudhuri and R. O. Pohl, Solid State Commun. 37, 105 (1980).

[17] C. A. Angell and D. B. Helphrey, J. Phys. Chem. 75, 2306 (1971).

[18] E. A. Porai-Koshits, J. Non-Cryst. Solids 25-26, 87 (1977); J. B. Bates, R. W. Hendricks, and L. B. Schaffer, J. Chem. Phys. 61, 4163 (1974).

[19] O. V. Mazurin, J. Non-Cryst. Solids 25-26, 130 (1977).

[20] Details in Ref. 12.

[21] R. D. Corsaro, Phys. Chem. Glasses 17, 2306 (1971).

[22] C. M. Gee and M. Kastner, Phys. Rev. Lett. 42, 1765 (1979).

[23] M. Kastner, J. Phys. C 13, 3319 (1980).

[24] M. H. Cohen and G. S. Grest, Phys. Rev. B 20, 1077 (1979).

[25] M. H. Cohen and G. S. Grest, Phys. Rev. Lett. 45, 1271 (1980); Solid State Commun. 39, 143 (1981).